

Acoustical and Optical Scattering and Imaging of Tissues – An Overview

Akira Ishimaru*

Department of Electrical Engineering, University of Washington

ABSTRACT

This talk will first give a general discussion on the ultrasound media characteristics of blood and spectral densities of tissues. The first-order scattering theory, multiple scattering theory, Doppler spectrum, cw and pulse scattering, focused beam, beam spot-size, speckle, texture, and rough interface effects will be presented. Imaging through tissues will then be discussed in terms of temporal and spatial resolutions, contrast, MTF (modulation transfer function), SAR and confocal imaging techniques, tomographic and holographic imaging, and inverse scattering. Next, we discuss optical diffusion in blood and tissues, radiative transfer theory, photon density waves, and polarization effects.

Keywords: Ultrasonic scattering and imaging in tissues and blood.

1. INTRODUCTION

For the past several decades, ultrasonic imaging has been studied extensively and a detailed historical account has been given in the excellent monograph by Shung and Thieme in 1993^[1]. We have also conducted research on several aspects of wave propagation and scattering in random media, and therefore, this paper presents an overview of some of the physical principles related to applications in ultrasound imaging of tissues and blood.

We start with ultrasound scattering in tissues, clarifying coherent and incoherent fields, multiple scattering effects, beam scattering, and pulse and interface effects. Next, we discuss ultrasound scattering by blood including Doppler, pulse scattering and beam scattering. We then focus on spatial and temporal resolutions including MTF, SAR, and confocal imaging. We will also add some discussions on optical diffusion in tissues and blood, and Wigner distributions.

2. ULTRASONIC SCATTERING IN TISSUES^{[1]-[6]}

For ultrasound, tissues can be considered “random continuum”, which means that the density ρ and the compressibility κ are continuous random functions of position. Under this assumption, we first obtain the scattering cross-section per unit volume of the tissue.

2.1 Ultrasonic tissue characteristics

Consider a volume δv of the tissues with the density ρ_e and the compressibility κ_e which are different from the surrounding average density ρ and compressibility κ . Under the assumption that the medium ρ_e and κ_e are only slightly different from ρ and κ , we can use the Born approximation to obtain the following well-known formula for the scattering amplitude:

$$f(\hat{o}, \hat{i}) = \frac{k^2}{4\pi} \int_{\delta v} (\gamma_\kappa + \gamma_\rho \cos\theta) e^{i\vec{k}_s \cdot \vec{r}'} dv' \quad (1)$$

where

$$\gamma_\kappa = \frac{\kappa_e - \kappa}{\kappa} = \text{compressibility fluctuation}$$

$$\gamma_\rho = \frac{\rho_e - \rho}{\rho_e} = \text{density fluctuation.}$$

* ishimaru@ee.washington.edu; phone 1 206 543-2169; fax 1 206 543-3842; <http://www.ee.washington.edu/people/faculty/ishimaru>;
Department of Electrical Engineering, University of Washington, Box 352500, Seattle, WA 98195-2500

We then obtain the differential scattering coefficient σ_d or the differential cross-section per unit volume of the tissue (Figure 1).

$$\sigma_d(\hat{o}, \hat{i}) = \frac{\langle ff^* \rangle}{\delta v} = \left(\frac{k^2}{4\pi}\right)^2 \frac{1}{\delta v} \iint \langle \gamma(\bar{r}_1)\gamma(\bar{r}_2) \rangle e^{i\bar{k}_s \cdot (\bar{r}_1 - \bar{r}_2)} dv_1 dv_2 \quad (2)$$

where

$$\gamma(\bar{r}) = \gamma_\kappa(\bar{r}) + \gamma_\rho(\bar{r}) \cos \theta$$

and

$$\bar{k}_s = k(\hat{i} - \hat{o}).$$

We can express (2) using the spectral densities

$$S_\gamma(\bar{k}_s) = \frac{1}{(2\pi)^3} \int B_\gamma(\bar{r}_d) e^{i\bar{k}_s \cdot \bar{r}_d} dv_d \quad (3)$$

and $B_\gamma(\bar{r}_d)$ is the correlation function given by

$$B_\gamma(\bar{r}_d) = \langle \gamma(\bar{r}_1)\gamma(\bar{r}_2) \rangle = B_\kappa(\bar{r}_d) + B_\rho(\bar{r}_d) \cos^2 \theta + 2 B_{\kappa\rho}(\bar{r}_d) \cos \theta. \quad (4)$$

We therefore have the expression for σ_d

$$\sigma_d(\hat{o}, \hat{i}) = \left(\frac{\pi}{2}\right) k^4 [S_\kappa(k_s) + S_\rho(k_s) \cos^2 \theta + 2 S_{\kappa\rho}(k_s) \cos \theta]. \quad (5)$$

The unit commonly used for σ_d (differential cross-section per unit volume) of the tissue is $cm^2/cm^3 sr = cm^{-1} sr^{-1}$ where sr = steradian (unit solid angle).

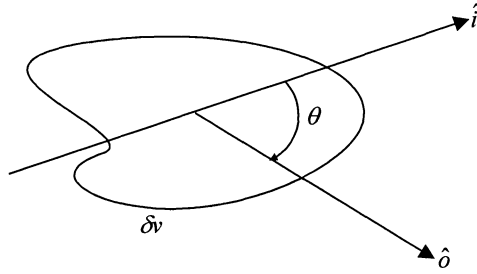


Figure 1: Incident wave is propagating in the direction \hat{i} (unit vector) and the scattered wave is observed in the direction \hat{o} (unit vector).

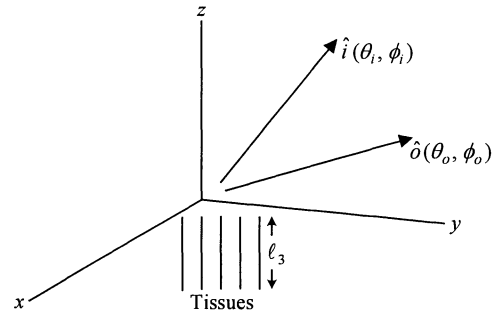


Figure 2: Anisotropic tissues.

2.1.1 Anisotropic tissue ^[2]

Tissues such as myocardium are often anisotropic. For example, they may be elongated in one direction. This can be expressed using Gaussian correlation function as:

$$B_\kappa(\bar{r}_d) = \sigma_\kappa^2 \exp\left(-\frac{x_d^2}{\ell_1^2} - \frac{y_d^2}{\ell_2^2} - \frac{z_d^2}{\ell_3^2}\right). \quad (6)$$

We can also assume that

$$\begin{aligned} B_\rho(\bar{r}_d) &\approx \frac{1}{2} B_\kappa(\bar{r}_d). \\ B_{\kappa\rho}(\bar{r}_d) &\approx 0. \end{aligned} \quad (7)$$

And typically, $\sigma_\kappa^2 \approx 10^{-4}$, $\ell_1 \approx \ell_2 \approx 30 \mu m$ and $\ell_3 \approx 200 \mu m$.

We then get (Figure 2)

$$S_{\kappa}(\bar{k}_s) = \frac{\sigma_{\kappa}^2 \ell_1 \ell_2 \ell_3}{8\pi\sqrt{\pi}} \exp\left[-\frac{1}{4}(k_{s1}^2 \ell_1^2 + k_{s2}^2 \ell_2^2 + k_{s3}^2 \ell_3^2)\right] \quad (8)$$

where

$$\begin{aligned} k_{s1} &= k(\sin\theta_i \cos\phi_i - \sin\theta_0 \cos\phi_0) \\ k_{s2} &= k(\sin\theta_i \sin\phi_i - \sin\theta_0 \sin\phi_0) \\ k_{s3} &= k(\cos\theta_i - \cos\theta_0). \end{aligned}$$

It is known that anisotropic tissues such as shown above exhibit the double peaks in the scattering pattern as shown in Figure 3.

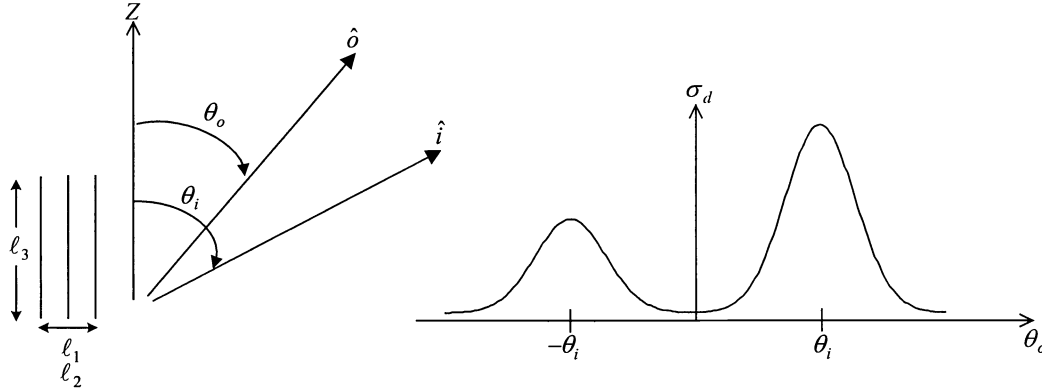


Figure 3: Differential Scattering Coefficient σ_d for anisotropic tissues.

2.1.2 Spectral density $S_{\kappa}(\bar{k}_s)$

The Gaussian spectrum (8) is often used since it is mathematically simple and includes the essential parameters σ_{κ} , ℓ_1 , ℓ_2 , and ℓ_3 . However, other spectra which may be more representative of the actual tissues have been proposed including fluid spheres, exponentials and modified exponentials. Here, we add the following power-law spectrum.

$$S_{\kappa}(\bar{k}_s) = S_{\kappa}(0) [1 + (k_{s1}\ell_1)^2 + (k_{s2}\ell_2)^2 + (k_{s3}\ell_3)^2]^{-n/2} \quad (9)$$

where k_{s1} , k_{s2} and k_{s3} are given in (8), and n is called “spectral index”.

If the spectral index n is 3, (9) reduces to the “Henye-Greenstein” formula and if $n = 4$, it reduces to the spectrum for the exponential correlation function. In general, for the isotropic case, we write

$$B(r_d) = B(0) \frac{1}{2^{\nu-1}\Gamma(\nu)} \left(\frac{r_d}{\ell}\right)^{\nu} K_{\nu}\left(\frac{r}{\ell}\right) \quad (10)$$

and

$$S(k_s) = B(0) \frac{\Gamma(\nu + \frac{3}{2})}{\pi\sqrt{\pi}\Gamma(\nu)} \frac{\ell^3}{(1 + k_s^2 \ell^2)^{\nu + \frac{3}{2}}}$$

valid when $\nu > -3/2$.

2.2 Coherent and incoherent waves ^[5]

As the pressure wave $p(\bar{r})$ propagates through a random medium such as tissue, the wave experiences random fluctuation in space and time, and becomes a random function. We can therefore express the wave as a sum of the coherent (average) $\langle p \rangle$ and incoherent (diffuse) p_d components

$$p = \langle p \rangle + p_d. \quad (11)$$

For a time harmonic wave with $\exp(-i\omega t)$ time dependence, we can express p in (11) in the complex plane (Figure 4).

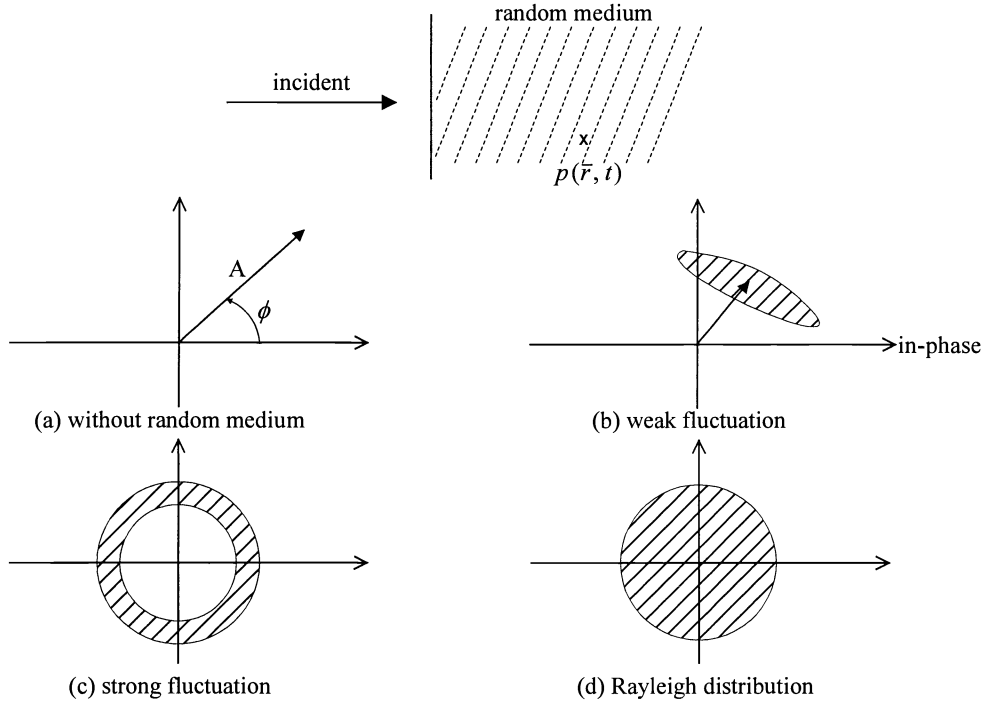


Figure 4: Coherent and Incoherent waves.

$$p = A e^{i\phi}. \quad (12)$$

As shown in Figure 4, if the randomness of the medium is small or the propagation distance is short, the wave first experiences phase fluctuations with small amplitude fluctuation (b). As the fluctuation increases, the phase fluctuation becomes significant (c). Eventually, however, both in-phase and quadrature components become Gaussian distributed, and this is called the “Rayleigh distribution”.

Let us first consider the coherent field $\langle p \rangle$. The total field p satisfies the wave equation.

$$(\nabla^2 + k^2)p = 0. \quad (13)$$

The wave number k is a random function and can be written as

$$k^2 = \langle k^2 \rangle (1 + \varepsilon) \quad (14)$$

where ε is the fluctuation.

The propagation characteristics of $\langle p \rangle$ have been studied extensively and given by the equivalent propagation constant K .

$$(\nabla^2 + K^2)\langle p \rangle = 0 \quad (15)$$

where

$$K^2 = \langle k^2 \rangle - \frac{i \langle k^2 \rangle^{3/2}}{2} \int_0^\infty dr \langle \varepsilon_1 \varepsilon_2 \rangle (e^{i2\langle k \rangle r} - 1)$$

where $\langle \varepsilon_1 \varepsilon_2 \rangle = \langle \varepsilon(r_1) \varepsilon(r_2) \rangle$

$$r = |r_1 - r_2|, \text{ and } \langle k \rangle = \langle k^2 \rangle^{1/2}.$$

Note that in general k is complex showing that the coherent field $\langle p \rangle$ attenuates due to the scattering.

If $\langle \varepsilon_1 \varepsilon_2 \rangle$ is exponential, then we have

$$K^2 = \langle k^2 \rangle \left[1 + \frac{\langle k^2 \rangle \ell^2 \sigma_\varepsilon^2}{1 - i2 \langle k \rangle \ell} \right] \quad (16)$$

showing attenuation (positive imaginary part).

The incoherent field p_d can be obtained by several formulations depending on the amount of fluctuations. For very weak fluctuations, we use the first-order scattering theory. As the fluctuations increase, the second-order and multiple scattering need to be considered. In the limit of many scattering, we have diffusion approximations (Figure 5).

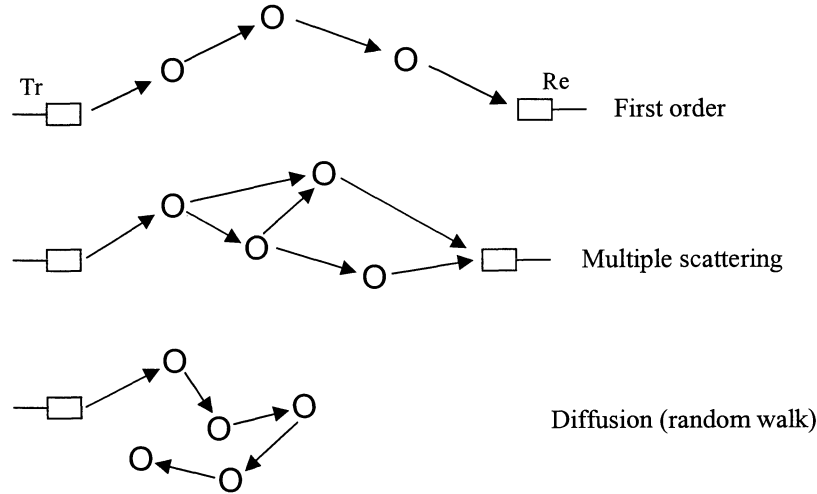


Figure 5: First order, multiple scattering, and diffusion.

2.3 Beam propagation and scattering

Let us consider a collimated Gaussian beam propagating in a random medium which is given by the Gaussian correlation function.

$$\langle \gamma(\vec{r}_1) \gamma(\vec{r}_2) \rangle = \sigma_\gamma^2 \exp\left(-\frac{\gamma_d^2}{\ell^2}\right). \tag{17}$$

The beam at $z = 0$ is given by

$$p(z = 0) = A_0 \exp\left[-\left(\frac{\rho}{w_0}\right)^2\right] \tag{18}$$

where $\rho^2 = x^2 + y^2$ and w_0 is the beam size (Figure 6).

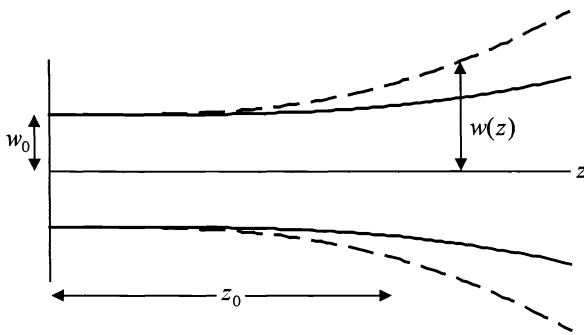


Figure 6: Collimated beam in random medium

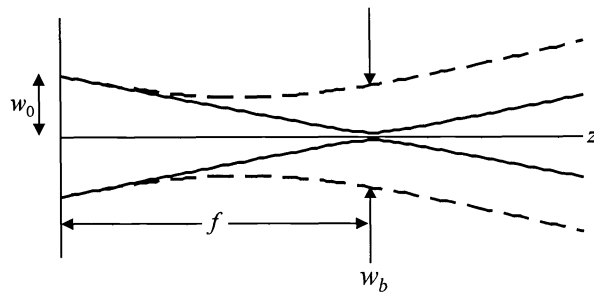


Figure 7: Spot size of focused beam

Due to the random medium, the total beam size is expanded, and the intensity at z is given by

$$I(z) = A_0^2 \frac{w_0^2}{w(z)^2} \exp\left[-\frac{2\rho^2}{w(z)^2}\right]. \quad (19)$$

The beam size $w(z)$ is given by

$$w(z) = w_0 \left[1 + \frac{z^2}{z_0^2} \left(1 + \frac{2}{3} \frac{\tau_0 w_0^2}{\ell^2} \right) \right]^{1/2} \quad (20)$$

where $z_0 = \frac{k w_0^2}{2}$, $\ell =$ correlation distance, $\tau_0 =$ optical depth $= \sqrt{\pi} (k^2 \sigma_r^2 \ell) z$.

This is pictured in Figure 6.

If the beam is focused at the focal distance f , then the beam spot size at $z = f$ is given by

$$w_b(z = f) = w_0 \left(\frac{f}{z_0} \right) \left[1 + \frac{2}{3} \tau_0 \left(\frac{w_0}{\ell} \right)^2 \right]^{1/2}. \quad (21)$$

2.4 Pulse propagation

Next we consider the propagation of a short pulse in a random medium. As the wave undergoes multiple scattering, the wave experiences time delay, and its cumulative effect is expressed by the pulse broadening (Figure 8). The broadening depends on the medium and the optical scattering depth and is approximately given by

$$T_c = \left(\frac{L}{C} \right) \frac{\tau_0^p}{2k^2 \ell^2} \quad (22)$$

where τ_0 is the optical scattering depth and ℓ is the correlation distance, p is a constant (1 to 2) depending on the medium correlation function, and $p = 1$ for Gaussian correlation function.

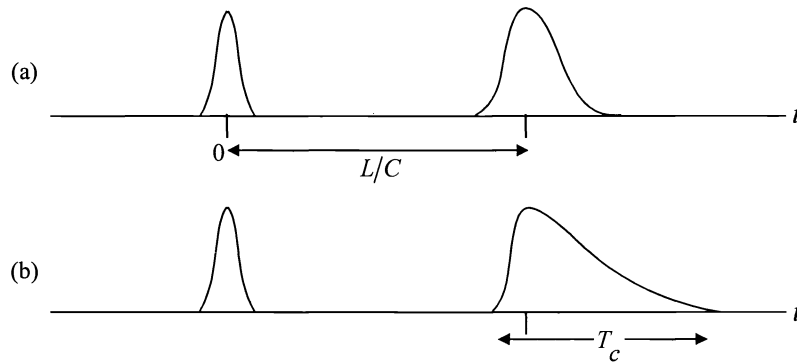


Figure 8: Pulse propagation for (a) weak fluctuation and (b) strong fluctuation.

2.5 Interface effects ^{[5][6]}

When a wave, which has propagated through a random medium, is incident on a rough interface, the scattered wave is modified by the roughness (Figure 9). If the surface is smooth, the reflected wave behaves in a manner similar to the incident wave. As the roughness increases, the diffuse components increase and the coherent component diminishes. The incident wave has already propagated through the random medium, and therefore it consists of the coherent and the incoherent waves. We express this by the incident specific intensity $I_i(\hat{i})$, which is a function of the direction \hat{i} . The scattered specific intensity $I_s(\hat{o})$ is then given by

$$I_s(\hat{o}) = \frac{1}{4\pi \cos \theta_s} \int \sigma^o(\hat{o}, \hat{i}) I_i(\hat{i}) d\omega_i \quad (23)$$

where σ^o is the scattering cross-section per unit area of the rough surface and $d\omega_i$ is the elementary solid angle for \hat{i} . If the surface is Lambertian, then, the cross-section is given by

$$\sigma^o(\hat{o}, \hat{i}) = \sigma_o \cos\theta_i \cos\theta_s. \quad (24)$$

And therefore,

$$I_s(\hat{o}) = \frac{\sigma_o}{4\pi} \int I_i \cos\theta_i d\omega_i. \quad (25)$$

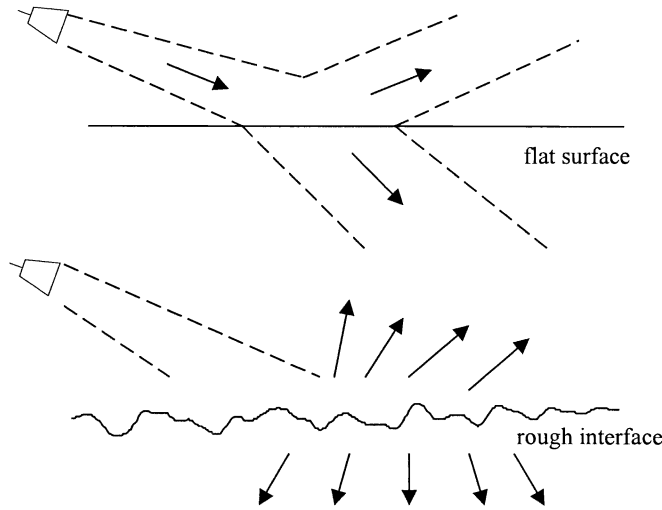


Figure 9: Reflection by flat and rough interfaces.

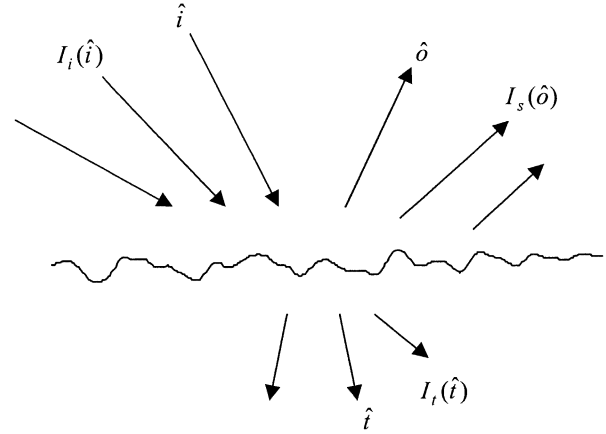


Figure 10: Specific intensities at the interface.

3. SCATTERING IN BLOOD, SCATTERING COEFFICIENTS, AND DOPPLER SHIFT

The ultrasonic scattering amplitude of a single red blood cell is well known [5].

$$f(\hat{o}, \hat{i}) = \frac{k^2 a^3}{3} \left(\frac{\kappa_e - \kappa}{\kappa} + \frac{3}{2} \frac{\rho_e - 3\rho}{\rho_e + 3\rho} \cos\theta \right) \quad (26)$$

where a is the radius of the equivalent spherical cell. The differential scattering cross-section per unit volume of the blood is therefore

$$\sigma(\hat{o}, \hat{i}) = \frac{H f_p(H)}{V_e} |f(\hat{o}, \hat{i})|^2 \quad (27)$$

where H is the hematocrit (0.4 for human), V_e is the volume of the single cell ($4\pi a^3/3$), and $f_p(H)$ is the packing factor [1]. The Percus-Yevick packing factor for hard spheres is often used as an approximation

$$f_p(H) = \frac{(1-H)^4}{(1+2H)^2}. \quad (28)$$

If the blood is moving with velocity \bar{V} which consists of the average $\langle \bar{V} \rangle = \bar{U}$ and the fluctuating velocity \bar{V}_f , then we have the cross-section with Doppler shift.

$$\sigma(\hat{o}, \hat{i}, \omega) = \sigma(\hat{o}, \hat{i}) \left[\frac{2\pi}{k_s^2 \sigma_f^2} \right]^{1/2} \exp \left[-\frac{(\omega + \bar{k}_s \cdot \bar{U})^2}{2k_s^2 \sigma_f^2} \right] \quad (29)$$

where we assumed the fluctuating velocity \bar{V}_f is Gaussian distributed, and $\bar{k}_s = k(\hat{i} - \hat{o})$.

4. IMAGING AND RESOLUTION

4.1 Modulation Transfer Function (MTF) ^{[5]-[7], [9]}

As a wave propagates through a random medium, the wave at any point is a mixture of coherent and incoherent waves. If we observe this wave with a lens or an array of detectors, we no longer obtain the Airy disk (Figure 11). The coherent intensity P_c is the Airy disk with its magnitude diminished by the optical depth $\exp(-\tau_o)$. The incoherent intensity P_i is spread out due to the angular spread $\Delta\theta$, which is related to the correlation distance (coherence length) ρ_o of the wave (Figure 12).

$$\Delta\theta \sim \frac{\lambda}{\rho_o} \sim \frac{1}{k\rho_o}. \quad (30)$$

The coherence length ρ_o is an important quantity not only giving the angular spread, but it also gives the pulse spreads Δt

$$\Delta t \sim \left(\frac{L}{C}\right) \frac{\Delta\theta^2}{2} \sim \left(\frac{L}{C}\right) \frac{1}{2k^2\rho_o^2} \quad (31)$$

where L is the propagation distance.

Note that the coherence length ρ_o is approximately given by

$$\rho_o \sim \frac{\ell}{\sqrt{\tau_o}} \text{ and } \tau_o \sim \sqrt{\pi} k^2 \sigma_r^2 \ell \text{ (tissues)}. \quad (32)$$

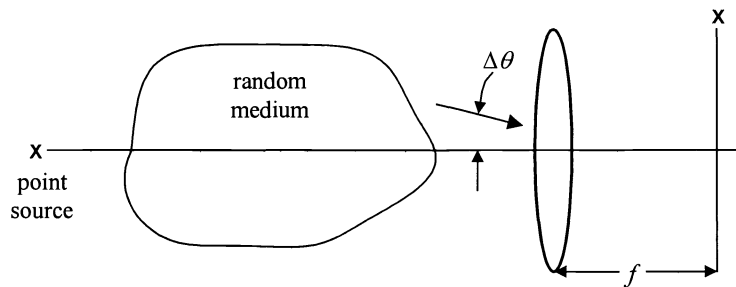


Figure 11: Image of a point source through random medium.

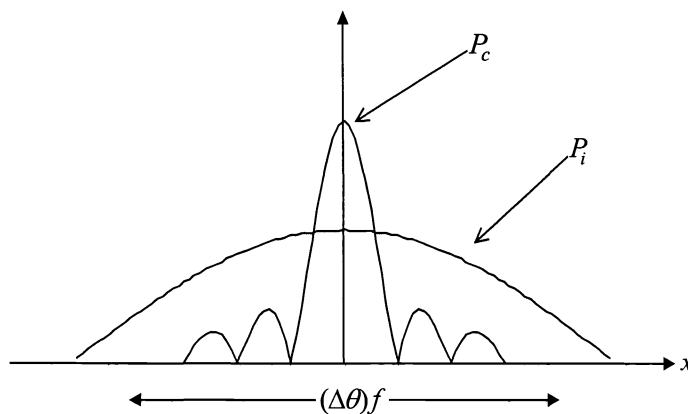


Figure 12: Airy disk P_c and incoherent intensity P_i

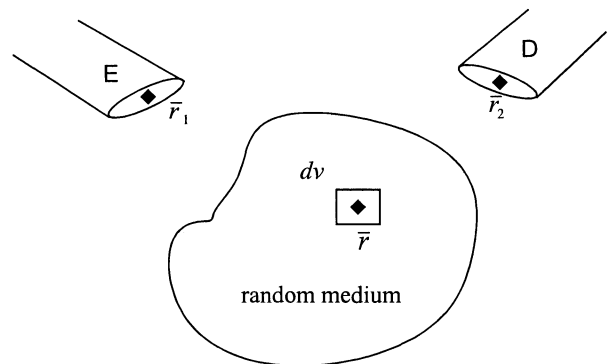


Figure 13: Wigner distribution

4.2 SAR and Confocal imaging

Synthetic aperture radar and confocal imaging techniques have been used extensively to obtain high resolution images. Conventional linear SAR can be generalized to circular or other SAR geometries^[12]. Confocal imaging is similar to SAR and has been used extensively in optical applications. It is also possible to make use of the signal processing techniques such as Capon's method. It has been shown that Capon's method combined with chirp pulse SAR can give an improved image, even under some multiple scattering environments.

5. OTHER IMAGING TECHNIQUES

Several other imaging techniques have been proposed, including the use of coherent backscattering^{[8][10][12]}, tomographic and holographic imaging, and speckle interferometry. In optical imaging for tissues, diffusion approximations are extensively used including photon density waves^[11], polarization, and pulse scattering.

6. WIGNER DISTRIBUTION

Let us formulate the problem of transmitting aperture, scattering medium, and receiving aperture (Figure 13). The formulation is similar to those given by Waag^[1], but makes use of the Wigner distribution. At the emitter E, the aperture distribution is given by $p_1(\bar{\rho}_1)$. The mutual coherence function at E is given by

$$\Gamma(\bar{\rho}_1, \bar{\rho}'_1) = \langle p_1(\bar{\rho}_1) p_1^*(\bar{\rho}'_1) \rangle \quad (33)$$

Wigner distribution $W(\bar{\rho}_c, \bar{k})$ is then obtained by

$$W(\bar{\rho}_c, \bar{k}) = \int \Gamma(\bar{\rho}_1, \bar{\rho}'_1) e^{i\bar{k} \cdot \bar{\rho}_d} d\bar{\rho}_d \quad (34)$$

where $\bar{\rho}_d = \bar{\rho}_1 - \bar{\rho}'_1$ and $\bar{\rho}_c = (\bar{\rho}_1 + \bar{\rho}'_1)/2$.

Note that W is similar to the specific intensity. The difference is that the specific intensity is real and positive, while the Wigner distribution can be negative.

Now, the Wigner distribution propagates through the random medium and at \bar{r} , we have $W_i(\bar{r}, \bar{k}_i)$ incident upon V . The scattered Wigner distribution $W_s(\bar{r}, \bar{k}_s)$ is then given by

$$W_s(\bar{r}, \bar{k}_s) = \int S_s(\bar{k}_s, \bar{k}_i) W_i(\bar{r}, \bar{k}_i) d\bar{k}_i \quad (35)$$

where S_s is the phase function.

The scattered Wigner distribution W_s then propagates through the random medium and reaches the detector D. The received power is then given by

$$P_r = \int A_r(\bar{r}_2, \bar{k}_s) W_s(\bar{r}_2, \bar{k}_s) d\bar{k}_s d\bar{r}_2 \quad (36)$$

where A_r is the Wigner distribution of the aperture distribution.

This formulation requires a detailed study of the propagation characteristics through the random medium such as those obtained by radiative transfer theory^[5].

7. CONCLUSION

In this paper, we presented an overview of the ultrasound imaging of tissues and blood. Included are general discussions on coherent and incoherent waves, beam, rough interface, speckle, MTF, SAR, optical diffusion, and Wigner distributions.

ACKNOWLEDGMENT

This work was supported by NSF (ECS 9908849).

REFERENCES

1. K.K. Shung and G.A. Thieme, *Ultrasonic Scattering in Biological Tissues*, CRC Press, Boca Raton, 1993.
2. M.F. Insana, "Modeling acoustic backscatter from kidney microstructure using an anisotropic correlation function," *J. Acoust. Soc. Amer.*, vol. 97, pp. 649-655, 1995.
3. M. F. Insana, R.F. Wagner, K. G. Brown, and T. J. Hall, "Describing small-scale structure in random media using pulse-echo ultrasound," *J. Acoust. Soc. Amer.*, vol. 87, pp. 179-192, 1990.
4. R. N. Czerwinski, D. L. Jones, and W. D. O'Brien, Jr., "Line and boundary detection in Speckle Images", *IEEE Trans. Image Processing*, vol 7, no 12, pp. 1700-1714, 1998.
5. A. Ishimaru, *Wave Propagation and Scattering in Random Media*, IEEE Press, Piscataway, New Jersey and Oxford University Press, Oxford, England, An IEEE-OUP Classic Reissue, 1997.
6. A. Ishimaru, *Electromagnetic Wave Propagation, Radiation, and Scattering*, Prentice Hall, New Jersey, 1991.
7. A. Ishimaru, "Limitation on image resolution imposed by a random medium," *Applied Optics*, 17:3, pp. 348-352, February 1978.
8. Y. Kuga and A. Ishimaru, "Retroreflectance from a dense distribution of spherical particles," *Journal of the Optical Society of America A*, 1:8, pp. 831-835, August 1984.
9. Y. Kuga and A. Ishimaru, "Modulation transfer function and image transmission through randomly distributed spherical particles," *Journal of the Optical Society of America A*, 2:12, pp. 2330-2336, December 1985.
10. A. Ishimaru, "Backscattering enhancement: From radar cross sections to electron and light localizations to rough surface scattering," *IEEE Antennas and Propagation Magazine*, 33:5, pp. 7-11, October 1991 (Invited Paper).
11. A. D. Kim and A. Ishimaru, "Optical diffusion of continuous-wave, pulsed, and density waves in scattering media and comparisons with radiative transfer," *Applied Optics*, 37:22, pp. 5313, August 1998.
12. A. Ishimaru, T.-K. Chan, and Y. Kuga, "An imaging technique using confocal circular synthetic aperture radar," *IEEE Transactions on Geoscience and Remote Sensing*, 36:5, pp. 1524-1530, September 1998.